# Investigation of the nature of the unpaired electron states in the organic semiconductor N-methyl-N-ethylmorpholinium-tetracyanoquinodimethane

**Rice, M. J.; Yartsev, V. M.; Jacobsen, Claus Schelde**

*Published in:*
Physical Review B Condensed Matter

*Link to article, DOI:*
10.1103/PhysRevB.21.3437

*Publication date:*
1980

*Document Version*
Publisher's PDF, also known as Version of record

PHYSICAL REVIEW B VOLUME 21, NUMBER 8 15 APRIL 1980

# Investigation of the nature of the unpaired electron states in the organic semiconductor N-methyl-N-ethylmorpholinium-tetracyanoquinodimethane

M. J. Rice
*Xerox Webster Research Center,* Webster, New York 14580*
*and Nordita, Copenhagen, Denmark*

V. M. Yartsev
*Fysisk Laboratorium III, Danmarks tekniske Højskole, DK-2800 Lyngby, Denmark*
*and Department of Physics,* Kuibyshev State University, Kuibyshev, Union of Soviet Socialist Republic**

C. S. Jacobsen
*Fysisk Laboratorium III, Danmarks tekniske Højskole, DK-2800 Lyngby, Denmark*
(Received 9 October 1979)

The nature of the unpaired electron states in the dimerized phase of the crystalline organic semiconductor N-methyl-N-ethylmorpholinium-tetracyanoquinodimethane [MEM(TCNQ)$_2$] is investigated by the combined means of polarized-optical-reflectance measurements and microscopic theoretical analysis. It is found that each unpaired electron is localized on a dimeric TCNQ unit, and it is demonstrated that the two-site molecular orbital (MO) which accommodates the unpaired electron involves internal molecular distortion of the dimeric unit. Experimental values are deduced for the intradimer $\pi$ MO hopping integral, the TCNQ monomer $a_g$ molecular-vibration frequencies and linear-electron-molecular-vibration coupling constants, and the difference in energy of the slightly nonequivalent TCNQ monomer $\pi$ MO's. The dimer charge oscillation associated with the extremely weak coupling of the unpaired electron to the high-frequency $a_g$ C–H stretch mode of the TCNQ molecule is observed for the first time.

## I. INTRODUCTION AND SYNOPSIS

Recently, the Gröningen group[1-4] has investigated the physical properties of the intermediate conductivity complex TCNQ salt N-methyl-N-ethylmorpholinium-tetracyanoquinodimethane MEM(TCNQ)$_2$. In common with all the compounds which belong to this interesting class of TCNQ salts the planar TCNQ molecules in MEM(TCNQ)$_2$ stack to form linear conducting chains.[5] Since MEM is present as a closed-shell cation in this salt, the chemical formula MEM(TCNQ)$_2$ indicates the formal presence of one-half of an unpaired electron on each TCNQ molecule. These electrons are accommodated by the $b_{2g}$ $\pi$ molecular orbital (MO) of the TCNQ molecule[6] and are responsible for the origin of electrical conductivity. Between 20 and 335 K, MEM(TCNQ)$_2$ exists in a triclinic crystalline phase in which the linear TCNQ chains are strongly dimerized with alternating interplanar distances of 3.15 and 3.27 Å.[2] The mode of the intradimer overlap is quite different from that of the interdimer overlap. These modes of overlap are illustrated in Figs. 1(a) and 1(b), respectively. The former favors a strong interaction of the $\pi$ MO's while the latter is indicative of a weak interaction of orbitals. These considerations point to a ground state in which the unpaired electrons singly occupy one-electron states which are predominantly localized on the dimers and weakly interacting with each other. Single occupancy, in the ground state, would be dictated by the Coulomb repulsion between the unpaired electrons. The magnitude and temperature ($T$) dependence of the observed paramagnetism is consistent with a linear array of localized unpaired spins subject to weak nearest-neighbor antiferromagnetic exchange coupling.[1,3] The magnitude of the activation energy,[4] $\Delta_\sigma \simeq 0.4$ eV for electrical conductivity $\sigma$ in the direction of the chain axis (crystal $c$ direction), is not inconsistent with the thermal promotion of mobile defect pairs, consisting of doubly occupied and unoccupied localized states. At room temperature $\sigma \simeq 10^{-2}(\Omega\ \mathrm{cm})^{-1}$.

At approximately $T = 335$ K MEM(TCNQ)$_2$ undergoes a transition to a new structural phase in which the TCNQ molecules are stacked almost uniformly.[4] The dc conductivity jumps discontinuously to about $30(\Omega\ \mathrm{cm})^{-1}$, and in the new phase is only weakly $T$ dependent. At low temperatures there is yet a third structural phase.[4] In the region of $T = 20$ K the unit cell of the dimerized phase doubles, leading to a tetramerized linear chain structure and loss of spin paramagnetism. The Gröningen workers have ascribed this transition to a spin-Peierls transition,[3,4] involving alternation in the interdimer spacing which, we note, is similar to that occurring in the complex salt triethylammonium (TEA)(TCNQ)$_2$ at room temperature.

The purpose of the present paper is to investi-

 

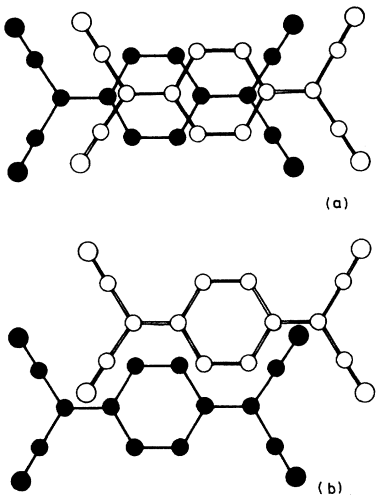


FIG. 1. Modes of TCNQ overlap in $MEM(TCNQ)_2$; (a) intradimer overlap, (b) interdimer overlap.

gate the nature of the unpaired electron states in the dimerized phase of $MEM(TCNQ)_2$. If each unpaired electron is localized on a dimeric TCNQ unit, the spectrum of low-lying excitations of $MEM(TCNQ)_2$ should be that of a radical-ion TCNQ dimer. A detailed theoretical description of this spectrum has been given recently by one of the present authors.[7] It consists of a primary electronic charge-transfer (CT) mode and a series of oscillations in the radical electron–electric dipole moment driven by the antisymmetric modes of internal molecular vibration of the dimer. The latter are a consequence[8] of the intramonomer electron-molecular-vibration (EMV) coupling and, for short, we shall refer to them as "dimer charge oscillations." The spectrum may be directly verified by means of polarized-optical-reflectance measurements. We report in this paper the results of such measurements taken on large single crystals of $MEM(TCNQ)_2$ at room temperature and in the optical range 50–30 000 $cm^{-1}$.

For application to $MEM(TCNQ)_2$, the existing theory[7] of the dimeric excitation spectrum requires a minor but interesting modification to allow for the slight inequivalence of the TCNQ monomers which constitute the dimeric unit in this compound. The inequivalence of the monomers is indicated by the observation[2] of slightly differing internal bond lengths and is a consequence of an asymmetric neighboring cation arrangement in $MEM(TCNQ)_2$. As we shall see later, however, such a source of site inequivalence will always trigger the occurrence of an additional inequivalence involving vibronic distortion. The modified theory, which does not alter the qualitative form of the excitation spectrum, is presented in this paper.

The experimentally measured excitation spectrum is found to be in complete accord with the theoretical spectrum. A definitive verification of the localized nature of the unpaired electron states in $MEM(TCNQ)_2$ is thus established. A detailed fit of the theory to the experimental spectrum enables experimental values to be deduced for the physical constants that appear in the microscopic theory. These are (a) the intradimer $\pi$ MO hopping or resonance integral $t$, (b) the TCNQ monomer $a_g$ molecular vibration frequencies $\{\omega_\alpha\}$, (c) the TCNQ monomer $a_g$ EMV coupling constants $\{g_\alpha\}$, and (d) the initial difference in energy $2\Delta_c$ of the inequivalent TCNQ monomer $\pi$ MO's. The significance of the experimental values obtained for these quantities to the question of EMV coupling in TCNQ salts is discussed.

It is remarkable that the dimer charge oscillation which is specifically associated with the coupling of the unpaired electron to the high-frequency $a_g$ CH–stretch mode ($\omega_1 = 3050$ $cm^{-1}$) of the TCNQ molecule is observed in the present measurements. The value of the appropriate dimensionless EMV coupling constant involved here, $\lambda_\alpha \simeq (g_\alpha^2/\omega_\alpha t)$, is of order $10^{-4}$, which is two orders of magnitude smaller than typical values. That there should exist an extremely small, but nevertheless, finite electronic coupling to the CH stretch mode was predicted theoretically some years ago by Lipari and Duke.[9] The experimental value we obtain for $g_\alpha$ is in excellent accord with their theoretical estimate of this quantity.

An interesting aspect of the one-electron state that accommodates the unpaired electron on the TCNQ dimer is that it involves *molecular distortion*. This is found to be a consequence of the *simultaneous* presence of the initial (steric) slight inequivalence of the monomer sites ($\Delta_c$) and the monomer EMV coupling. In the absence of both of the latter factors the unpaired electron is shared equally among the two TCNQ monomers in a two-site bonding MO of energy $-t$, relative to the energy of the noninteracting TCNQ monomer $\pi$ MO. With the introduction of $\Delta_c$ (alone) the familiar secular determinant is modified to

$$\begin{vmatrix} E-\Delta_c & t \\ t & E+\Delta_c \end{vmatrix} = 0$$

and the energy $E$ of the bonding MO becomes $E = -(t^2+\Delta_c^2)^{1/2}$, indicating an increased stability with respect to the former energy of $-t$. Now however, the unpaired electron is not shared

equally among the two monomer sites; its charge density is slightly greater at the monomer site with energy $-\Delta_c$ than at the site with energy $\Delta_c$. But with the introduction of the monomer EMV coupling, an increase or decrease in charge density at a monomer site will lead to a lowering $-\Delta_v$, or raising $\Delta_v$ of the monomer $\pi$ MO as the internal bond lengths readjust to the new local charge densities. The inequivalence of the monomer sites is therefore further enhanced, leading to an even more stabilized two-site bonding orbital. This process of increased stability is, however, counterbalanced by the elastic restoring forces associated with the internal molecular distortion. In the ensuing text of this paper it will be seen that the sum of the electronic and molecular distortion energies of the dimeric system is

$$E_D = -[t^2+(\Delta_c+\Delta_v)^2]^{1/2}+\tfrac{1}{4}\sum_\alpha \omega_\alpha q_\alpha^2 , \qquad (1.1)$$

where $\Delta_c=\sum_\alpha (g_\alpha/\sqrt{2})\, q_\alpha$ and $\{q_\alpha\}$ denote a set of distortion coordinates (defined explicitly in Sec. II). Minimization of (1.1) with respect to the latter determine the equilibrium values $\{q_\alpha^0\}$ of the distortion and hence of the additional distortion "gap" $\Delta_v^0=\sum_\alpha (g_\alpha/\sqrt{2})q_\alpha^0$. The energy of the two-site bonding MO is finally $E=-[t^2+(\Delta_c+\Delta_v^0)^2]^{1/2}$. We shall refer to this electronic state as a "distorted dimer state."[10] The steps of its evolution are illustrated schematically in Fig. 2. Examination of (1.1) reveals that there will *always* occur a nonvanishing distortion ($q_\alpha^0 \neq 0$) provided that $\Delta_c$ is finite ($\Delta_c \neq 0$). For vanishing $\Delta_c$, no molecular distortion is possible—unless however, the quantity $E_p=\sum_\alpha (g_\alpha^2/\omega_\alpha)$ exceeds the energy $t$. The initial inequivalence $\Delta_c$ plays, therefore a *catalytic* role in the formation of the distortion gap $\Delta_v^0$.

Our paper is organized as follows. In Sec. II we present the microscopic theory of the unpaired electron state and apply it to derive a theoretical formula for the frequency-dependent electrical conductivity of a system of $N$ noninteracting ion-radical dimers. In Sec. III the procedure and results of our polarized-optical-reflectance measurements on MEM(TCNQ)$_2$ are presented. The theoretical analysis of the experimental data is presented and discussed in Sec. IV. The main conclusions of the paper are summarized in a final section.

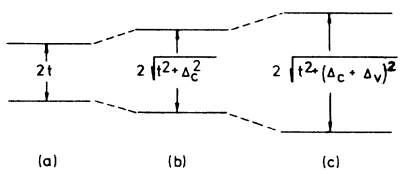


FIG. 2. Steps of evolution of the distorted dimer state; one-electron energy levels of the dimeric unit with (a) no site inequivalence, (b) steric-site inequivalence, and (c) steric-site inequivalence and vibronic coupling.

## II. MICROSCOPIC THEORY OF THE DISTORTED DIMER

The microscopic model which we will employ to describe the one-electron states of the ion-radical dimer is defined by the following Hamiltonian ($\hbar=1$):

$$H=H_e+H_v+\sum_{\alpha,i} g_\alpha n_i Q_{\alpha,i}-\vec{F}\cdot\vec{p}\,, \qquad (2.1)$$

where

$$H_e=(E_0+\Delta_c)n_1+(E_0-\Delta_c)n_2 + \sum_\sigma t(c_{2,\sigma}^\dagger c_{1,\sigma}+c_{1\,\sigma}^\dagger c_{2,\sigma})\,, \qquad (2.2)$$

$$H_v=\sum_{i,\alpha}\tfrac{1}{4}(\Pi_{\alpha,i}^2+Q_{\alpha,i}^2)\omega_\alpha\,, \qquad (2.3)$$

$$\vec{p}=\tfrac{1}{2}e\vec{a}(n_1-n_2)\,; \qquad (2.4)$$

$H_e$ is the Hamiltonian of the unpaired electron in the absence of vibronic coupling and consists of the interaction of the two monomer $\pi$ MO's. $(E_0+\Delta_c)$ denotes the energy of the (unperturbed) $\pi$ MO of monomer 1, while $(E_0-\Delta_c)$ denotes that for monomer 2. These energies are assumed to differ slightly ($\Delta_c \ll E_0$) on account of an asymmetric cation arrangement in the molecular crystal. $E_0$ is the common MO energy that would result in the absence of the asymmetric cation arrangement. $c_{i,\sigma}^\dagger$ and $c_{i,\sigma}$ denote site fermion creation and destruction operators for the unpaired electron, $i$ labeling the monomer site ($i=1,2$) and $\sigma$ the electronic spin. $n_i=\sum_\sigma c_{i,\sigma}^\dagger c_{i,\sigma}$ is the occupation number operator for the site $i$ and $t$ the $\pi$-MO hopping integral operating between the two monomer sites.

$H_v$ is the Hamiltonian of the totally symmetric ($a_g$) internal modes of vibration of the monomers and the third term of (2.1) describes their (linear) coupling to the monomer $\pi$ MO. $Q_{\alpha,i}$ denotes the (dimensionless) normal mode coordinate corresponding to the symmetric vibration $\alpha$ ($\alpha=1,2,\ldots,G$) of the monomer $i$, while $\omega_\alpha$ denotes its corresponding normal mode frequency. The set of $G$ constants $\{g_\alpha\}$ denote the $a_g$ monomer $\pi$-electron-molecular vibration (EMV) coupling constants.[11] In terms of the familiar vibrational creation ($a_{\alpha,i}^\dagger$) and destruction ($a_{\alpha,i}$) operators, we note that $Q_{\alpha,i}=a_{\alpha,i}+a_{\alpha,i}^\dagger$ and $\Pi_{\alpha,i}=a_{\alpha,g}-a_{\alpha,i}^\dagger$. For the TCNQ monomer, $G=10$, and the magnitudes of the $a_g$ frequencies span the wide range 140–3050 cm$^{-1}$.

The last term in (2.1) describes the interaction

of the unpaired electron with an externally applied electric field $\vec{F}$. The operator $\vec{p}$, defined by Eq. (2.4), denotes the electric dipole moment of the dimer due to the presence of the unpaired electron. In Eq. (2.4) the vector length $\vec{a}$, whose magnitude will be of the order of the intermonomer separation, is specified in practice by the mode of the dimeric overlap.[7] [In MEM(TCNQ)$_2$, for example, $\vec{a}$ will be the intermonomer spacing in the direction of the crystal $c$ axis].

The Hamiltonian (2.1) is similar to that studied by Rice[7] for the ion-radical dimer with two unpaired electrons. In that study the site nonequivalence $\Delta_c$ was absent but it was necessary to allow for the on-site Coulomb repulsion $U$ acting between the two unpaired electrons when occupying the same MO. For the present one-electron system the latter complication does not arise. Instead, we have the complication of $\Delta_c$ and to treat this problem it will be convenient to follow the analysis of Ref. 7.

We introduce the dimeric normal mode coordinates $q_\alpha = 2^{-1/2}(Q_{\alpha,1} - Q_{\alpha,2})$ and $s_\alpha = 2^{-1/2}(Q_{\alpha,1} + Q_{\alpha,2}) - s_\alpha^0$, with $s_\alpha^0 = -2^{1/2} g_\alpha/\omega_\alpha$ and the "charge-difference" operator $\delta n = n_1 - n_2$. Then noting that $N = n_1 + n_2$ is a constant of motion, equal to unity, the Hamiltonian (2.1) may be reexpressed as

$$H = H_e' + H_s + \sum_\alpha \tfrac{1}{4}(\pi_\alpha^2 + q_\alpha^2)\omega_\alpha + \sum_\alpha (g_\alpha/\sqrt{2})\delta n q_\alpha - \tfrac{1}{2}\vec{F}\cdot\vec{a}e\delta n\,, \tag{2.5}$$

where $H_e'$ is given by Eq. (2.2) with the replacement $E_0 \to E_0 - \frac{1}{2}E_p$, where $E_p = \sum_\alpha g_\alpha^2/\omega_\alpha$ is the conventionally defined "small-polaron" binding energy, and $H_s$ is the harmonic Hamiltonian $H_s = \sum_\alpha \frac{1}{4}(\sigma_\alpha^2 + s_\alpha^2)\omega_\alpha$ for the symmetric normal modes $s_\alpha$ ($\sigma_\alpha$ and $\pi_\alpha$ denote the dimensionless canonical momenta coordinates conjugate to $s_\alpha$ and $q_\alpha$, respectively). Equation (2.5) shows that the modes $s_\alpha$ are completely decoupled from the radical electron. They correspond to in-phase oscillations of the $a_g$ modes of the two monomers and their frequencies are just $\omega_\alpha$. These frequencies may be measured in Raman-scattering experiments.

Now the equations of motion for the antisymmetric modes $q_\alpha$ are

$$\ddot{q}_\alpha + \omega_\alpha^2 q_\alpha = -2^{1/2} g_\alpha \omega_\alpha \delta n\,. \tag{2.6}$$

Because of the nonequivalence of the monomer sites, the Hamiltonian (2.5) indicates a ground-state average of $\delta n$, $\langle\delta n\rangle$, that is nonvanishing. According to (2.6) this will imply a nonvanishing equilibrium value

$$q_\alpha^0 = -2^{1/2}(q_\alpha/\omega_\alpha)\langle\delta n\rangle \tag{2.7}$$

for the modes $q_\alpha$, i.e., the occurrence of internal molecular distortion. That this distortion leads to a further nonequivalence of the monomer sites may be seen by substituting the definitions $\delta q_\alpha = q_\alpha - q_\alpha^0$, $\delta\hat{n} = \delta n - \langle\delta n\rangle$ into the Hamiltonian (2.5). Ignoring the Hamiltonian $H_s$, (2.5) becomes

$$H = H_0 + H_{\rm int}\,, \tag{2.8}$$

where

$$H_0 = (\Delta_c + \Delta_v)\delta n + V_{12} + \tfrac{1}{4}\sum_\alpha \omega_\alpha (q_\alpha^0)^2 + \tfrac{1}{4}\sum_\alpha \omega_\alpha(\delta\pi_\alpha^2 + \delta q_\alpha^2) - \vec{F}\cdot\vec{p}^0 + E_0 - \tfrac{1}{2}Ep \tag{2.9}$$

and

$$H_{\rm int} = \left[\left(\sum_\alpha (g_\alpha/\sqrt{2})\delta q_\alpha\right) - \tfrac{1}{2}\vec{F}\cdot\vec{a}e\right]\delta\hat{n}\,. \tag{2.10}$$

In (2.9) $V_{12}$ denotes the third term of (2.2),

$$\Delta_V = 2^{-1/2}\sum_\alpha g_\alpha q_\alpha^0 \tag{2.11}$$

and $\vec{p}^0 = \frac{1}{2}e\vec{a}\langle\delta n\rangle$. The term $-\vec{F}\cdot\vec{p}^0$ in $H_0$ is assumed to be cancelled by an equal and opposite energy arising from the asymmetric cations, i.e., the total equilibrium electric dipole moment of the crystalline unit cell is assumed to be zero. Equation (2.9) and (2.11) reveal that the site nonequivalence is increased from $\Delta_c$ to $\Delta = \Delta_c + \Delta_V$.

The electronic part of the Hamiltonian (2.9) leads to a ground-state (bonding) eigenfunction for the unpaired electron

$$|E_-\rangle = c_1|\phi_1\rangle + c_2|\phi_2\rangle\,, \tag{2.12}$$

with eigenvalue[12] $E_- = -(t^2 + \Delta^2)^{1/2}$, and to an excited-state (antibonding) eigenfunction

$$|E_+\rangle = c_2|\phi_1\rangle - c_1|\phi_2\rangle\,, \tag{2.13}$$

with eigenvalue $E_+ = (t^2 + \Delta^2)^{1/2}$. In (2.13) and (2.14) $|\phi_i\rangle$ denotes the noninteracting $\pi$ MO of the monomer $i$ and the coefficients $c_i$ are

$$c_1 = (1 + h_-^2)^{-1/2},\quad c_2 = (1 + h_+^2)^{-1/2}\,, \tag{2.14}$$

in which

$$h_\pm = t/[\Delta \pm (\Delta^2 + t^2)^{1/2}]\,. \tag{2.15}$$

The Hamiltonian $H_{\rm int}$, defined by Eq. (2.10), describes a weak coupling between the states $|E_-\rangle$ and $|E_+\rangle$ resulting from the applied field $\vec{F}$ and from the fluctuations $\delta q_\alpha$ in the antisymmetric vibrational coordinates $q_\alpha$. This coupling will be treated in our subsequent derivation of the excitation spectrum of the dimer.

In order to calculate the equilibrium distortion values $\{q_\alpha^0\}$ and hence, the magnitude of $\Delta_v$, Eq. (2.7) is to be evaluated with respect to the ground-state eigenfunction (2.12). This leads to the set

of simultaneous nonlinear equations

$$q_\alpha^0 = \sqrt{2}\,(g_\alpha/\omega_\alpha)[\Delta/(t^2+\Delta^2)^{1/2}] \quad (\alpha = 1,2,\ldots,G)\,. \tag{2.16}$$

These equations also follow from minimizing the ground-state average of $H_0$ with respect to $q_\alpha^0$ [cf. Eq. (1.1) of the Introduction]. For the evaluation of the equilibrium value of $\Delta_v$, $\Delta_v^0$, it is not necessary, however, to solve (2.16) for the individual values of $q_\alpha^0$, for if both sides of Eq. (2.16) are multiplied by $(g_\alpha/\sqrt{2}\,)$ and then summed over $\alpha$, we directly obtain the result

$$\Delta_v^0 = E_p(\Delta_c+\Delta_v^0)/[t^2+(\Delta_c+\Delta_v^0)^2]^{1/2}\,, \tag{2.17}$$

or,

$$\Delta = \Delta_c + E_p\Delta/(t^2+\Delta^2)^{1/2}\,, \tag{2.18}$$

for the required total gap $\Delta = \Delta_c + \Delta_v^0$. As discussed in Sec. I, the solution of (2.17) or (2.18) will always yield $\Delta > \Delta_c$, i.e., $\Delta_v^0 \neq 0$, provided $\Delta_c \neq 0$. If $\Delta_c = 0$, a nonvanishing solution for $\Delta_v^0$ can arise only if $E_p > t$.

The Hamiltonian (2.9) describes $G+1$ noninteracting elementary excitations. These are the electronic charge-transfer (CT) excitation, $|E_-\rangle \rightarrow |E_+\rangle$, of frequency $\omega_{CT} = 2(t^2+\Delta^2)^{1/2}$, and the set of $G$ antisymmetric vibrations with frequencies $\{\omega_\alpha\}$. The first term of the Hamiltonian (2.10) shows that these excitations are linearly coupled to each other. If this term is compared with the second term of (2.10) it may be concluded that the fluctuations $\delta q_\alpha$ introduce the effective oscillating electric fields $\vec{F}_\alpha = (\sqrt{2}\,\vec{a}/ea^2)g_\alpha\delta q_\alpha$. These fields will drive small amplitude oscillations in the charge difference $\delta n$ and will also lead to a slight enhancement of the CT excitation frequency $\omega_{CT}$. As discussed in Ref. 7 and elsewhere,[8] the frequencies $\Omega_\alpha$ of the $G$ "dimer charge oscillations" and the renormalized frequency $\Omega_{CT}$ of the CT excitation, may be shown, within the framework of linear response theory, to be given by the $G+1$ solutions of the equation

$$\mathrm{Re}[\tilde{\chi}(\omega)D(\omega)] = 1\,, \tag{2.19}$$

where $\tilde{\chi}(\omega) = \chi(\omega)/\chi(0)$;

$$\chi(\omega) = |\langle E_+|\delta\hat{n}|E_-\rangle|^2 2\omega_{CT}/(\omega_{CT}^2-\omega^2-i\omega\gamma_e) \tag{2.20}$$

is the reduced CT electronic polarizability in the absence of vibronic coupling, and

$$D(\omega) = \sum_\alpha \lambda_\alpha\omega_\alpha^2/(\omega_\alpha^2-\omega^2-i\omega\gamma_\alpha)\,. \tag{2.21}$$

In (2.21), $\lambda_\alpha = E_p^\alpha\chi(0)$ characterizes the strengths of the individual CT excitation-molecular vibration couplings, where $E_p^\alpha = g_\alpha^2/\omega_\alpha$. In (2.20) and (2.21), $\gamma_e$ and $\gamma_\alpha$ denote phenomenological natural widths of the originally uncoupled CT excitation and antisymmetric vibration mode $\alpha$, respectively. The $G$ dimer charge oscillations—which, essentially, are the modes $\delta q_\alpha$ renormalized—and the renormalized CT excitation $\Omega_{CT}$, constitute the elementary excitations of the ion-radical dimer.

The frequency-dependent conductivity $\sigma(\omega)$ of a system of $N$ such dimers, arbitrarily positioned and noninteracting with each other, has been derived to be[7]

$$\vec{\sigma}(\omega) = \sigma(\omega)\vec{A}\,, \tag{2.22}$$

$$\sigma(\omega) = -i\omega\tfrac{1}{4}e^2a^2(N/\Omega)\chi(\omega)/[1-\tilde{\chi}(\omega)D(\omega)]\,, \tag{2.23}$$

$$\vec{A} = N^{-1}\sum_j(\vec{a}_j\vec{a}_j/a^2)\,. \tag{2.24}$$

In (2.23) $\Omega$ denotes the volume of the system and the quantity $\vec{A}$, in which the unit vector $\vec{a}_j/a$ specifies the orientation of the dimer $j$ ($j = 1,2,\ldots,N$), determines the tensorial character of $\vec{\sigma}(\omega)$. For a linear chain of dimers, such as occurs in MEM(TCNQ)$_2$, $\vec{A}_{\alpha\beta} = \delta^{Kr}_{\alpha c}\cdot\delta^{Kr}_{\beta c}$, where $c$ denotes the chain axis and $\delta^{Kr}$ is the Kronecker delta. In this case $\vec{\sigma}(\omega)$ is polarized along the chain axis with magnitude $\sigma(\omega)$.

Expression (20) for $\chi(\omega)$ may be evaluated with the use of Eqs. (2.12), (2.13), and (2.14) to be

$$\chi(\omega) = (8t/\omega_{CT})/(\omega_{CT}^2-\omega^2-i\omega\gamma_e)\,. \tag{2.25}$$

Consequently, for the linear-chain system, it follows from (2.23) and (2.25) that the dielectric constant $\epsilon(\omega)$ along the $c$ direction will be

$$\epsilon(\omega) = \epsilon_\infty + \frac{4\pi e^2a^2(N/\Omega)(2t^2/\omega_{CT})}{\omega_{CT}^2[1-D(\omega)]-\omega^2-i\omega\gamma_e}\,. \tag{2.26}$$

A constant dielectric constant $\epsilon_\infty$, has been introduced to account for the effect of the remaining high-frequency electronic transitions of the molecular constituents of the crystal.

## III. EXPERIMENTAL PROCEDURE AND RESULTS

Reflectance data at near normal incidence were obtained from MEM(TCNQ)$_2$ samples with well-shaped optical faces of approximate size $1\times5$ mm$^2$. The chain direction (crystallographic $c$ axis) was parallel to the long dimension of the samples.

Far-infrared data in the range 50–400 cm$^{-1}$ were taken with an RIIC FS720 Michelson interferometer equipped with a Cambridge Physical Sciences IGP220 polarizer. To obtain an acceptable signal-to-noise ratio in the far infrared, samples consisting of mosaics of aligned crystals were used. Absolute values were obtained by recording background spectra from sample mosaics covered with gold film. The spectral reso-

lution was ~3 $cm^{-1}$

Measurements in the intermediate infrared (400–4000 $cm^{-1}$) were done on a single-beam reflectometer based on a Perkin Elmer (PE) 98 grating monochromator and with a PE gold grid polarizer mounted in front of the sample. Absolute values of reflectance were determined by covering part of the samples with an aluminum film and comparing the signals from the naked and covered parts. Corrections for the finite reflectance of aluminum have been made. The spectral resolution in the range of sharp molecular resonances was below 10 $cm^{-1}$. Several lines were scanned with higher resolution to ensure that the correct linewidths were obtained. The measurements were continued to 30 000 $cm^{-1}$ using a PE98 quartz prism monochromator and a Nicol prism polarizer. In this high-frequency range, above all molecular vibration frequencies, the employed spectral resolution was fairly low: 200–500 $cm^{-1}$.

The overall accuracy in the absolute values of reflectance is estimated to be about 2%. The accuracy in the relative spectral dependence is somewhat better, perhaps about 1%.

In Fig. 3 we present the measured reflectance data. The frequency range is 50–30 000 $cm^{-1}$ for $R_{\parallel}$ (along the TCNQ stacks) and 50–16 000 $cm^{-1}$ for $R_{\perp}$ (perpendicular to the stacks).

$R_{\parallel}$ shows a typical electronic absorption around 3500 $cm^{-1}$, no doubt associated with the radical electron-charge-transfer excitations along the stacks. At higher frequencies a weak doublet appears around 10 000 $cm^{-1}$. The origin of this 10 000-$cm^{-1}$ absorption is controversial,[13] but it may arise from intramolecular absorption processes in the TCNQ molecule, since it is found at the same position in most TCNQ chain compounds.[14] The weak structure at higher frequencies is definitely intramolecular in origin.

Below the charge-transfer band, extremely strong lines are seen in the range of molecular vibrations. An analysis of these lines and of the 3500-$cm^{-1}$ absorption, based on the microscopic theory of Sec. II will be presented in the following section.

$R_{\perp}$ in contrast is flat with a strength in the molecular lines typical for a molecular crystal. The overall level is 7–8%, as commonly found in TCNQ salts along the low-conductivity directions. The monitoring of $R_{\perp}$ provides a direct check of polarizer efficiency. Note for example, that the very sharp drop in $R_{\parallel}$ near 1350 $cm^{-1}$ is not visible in $R_{\parallel}$ at all. Hence, the vibrational structure which coincides in $R_{\perp}$ and $R_{\parallel}$ can be fully trusted.

For use in the imminent theoretical analysis of the data, we have performed a dispersion analysis of $R_{\parallel}$ to obtain the frequency-dependent conductivity $\sigma(\omega)$ (Fig. 4). The required extrapolations consisted of assuming $R_{\parallel}$ constant and equal to 27% below 50 $cm^{-1}$, and 5.0% above 30 000 $cm^{-1}$. A change in extrapolation procedure will only give insignificant changes in $\sigma(\omega)$ in the range of principal interest. The extrapolation $R_{\parallel} = 27\%$

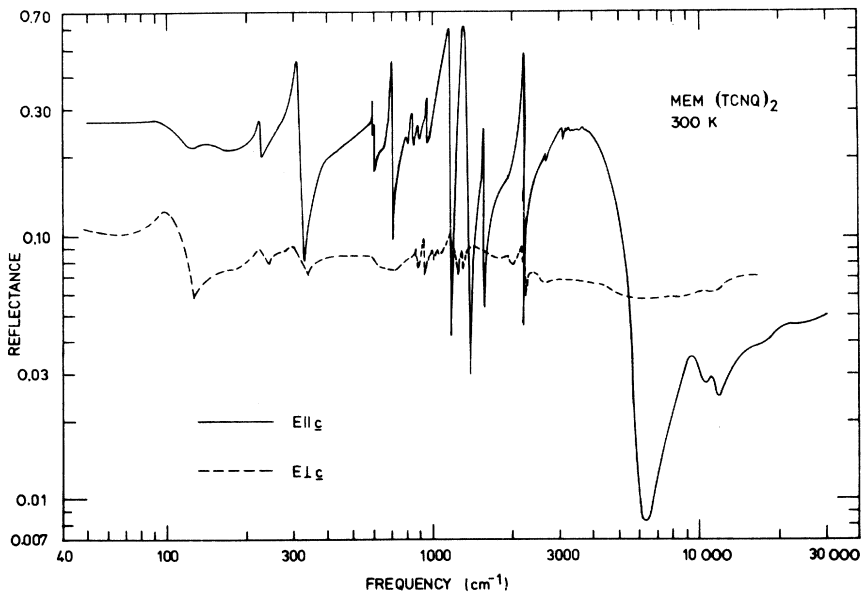


FIG. 3. The measured polarized optical reflectance of MEM$(TCNQ)_2$ at room temperature; full curve: electric field vector parallel to crystallographic $c$ axis; broken curve: electric field vector perpendicular to $c$ axis.

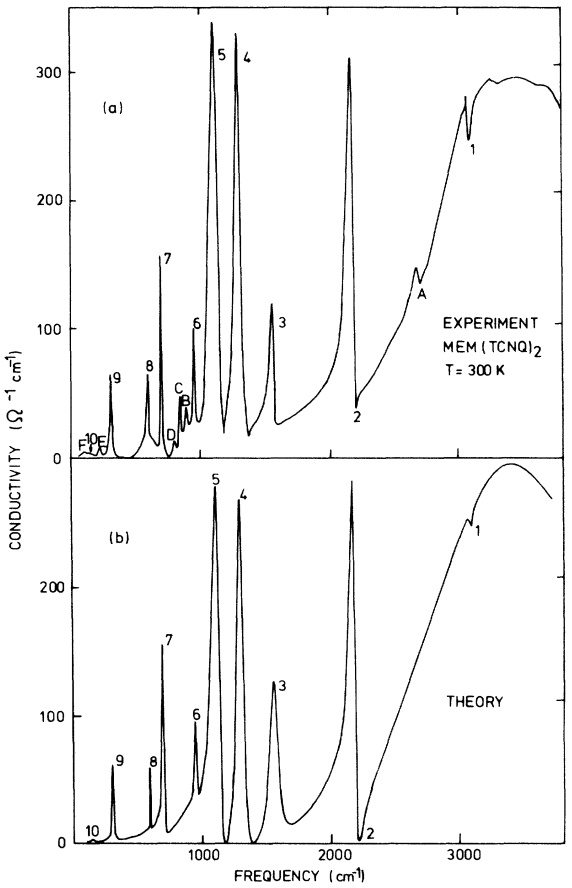


FIG. 4. Real part of the frequency-dependent conductivity along the crystallographic $c$ axis, as deduced by dispersion analysis of the measured reflectivity (upper curve) and calculated on the basis of the microscopic theory of Sec. II.

below 50 cm$^{-1}$ implies a static dielectric constant $\epsilon(0)=10$ along the chain direction. This value of $\epsilon(0)$ is in agreement with microwave measurements undertaken by the Gröningen group.[15]

## IV. ANALYSIS AND DISCUSSION

The experimentally determined real part of the frequency-dependent conductivity $\sigma(\omega)$ in the spectral range 50–3500 cm$^{-1}$, deduced from our measurement of $R_{\parallel}$, is shown in the upper portion of Fig. 4. The spectrum of elementary excitations revealed by $R(\sigma(\omega))$ is consistent with that expected for the ion-radical dimer. The broad electronic absorption centered about 3500 cm$^{-1}$ may be interpreted as the primary electronic CT excitation band, implying $\Omega_{CT} \simeq 3500$ cm$^{-1}$. The molecular absorption features, labeled 1 through 10, may be interpreted as the ten dimer charge-oscillation bands. A theoretically calculated spectrum, provided by Eqs. (2.23) and (2.25), is shown in the lower portion of Fig. 4. It would appear to confirm the dimer interpretation beyond reasonable doubt.

The latter theoretically calculated spectrum actually is a fit of Eqs. (2.23) and (2.25) to the experimental $R(\sigma(\omega))$ vs $\omega$ data. It was accomplished as follows. Three independent physical constants characterize a given absorption feature: its position along the $\omega$ axis, its (integrated) intensity, and its absolute height. Since we seek to fit a spectrum consisting of $G+1$ absorption features, we are required to furnish a total of 3 $(G+1)$ independent physical parameters. We chose these parameters to be $\{\omega_\alpha, \lambda_\alpha, \gamma_\alpha\}$ (for the $G$-dimer charge oscillations) and $\omega_{CT}$, $t^2/\omega_{CT}$, and $\gamma_e$ (for the primary CT band). These parameters were varied so as to obtain an optimum fit of Eqs. (2.23) and (2 25) to the experimental data. The values, $a=3.34$ Å and $N/\Omega = 1.4\times 10^{21}$ cm$^{-3}$, known from the crystal structure,[2] were employed in Eq. (2.23).

The optimum values found for the parameters were employed in Eq. (2.26) for $\epsilon(\omega)$ in order to calculate $R_{\parallel}(\omega)$. With the value $\epsilon_\infty = 1.8$ the cal-

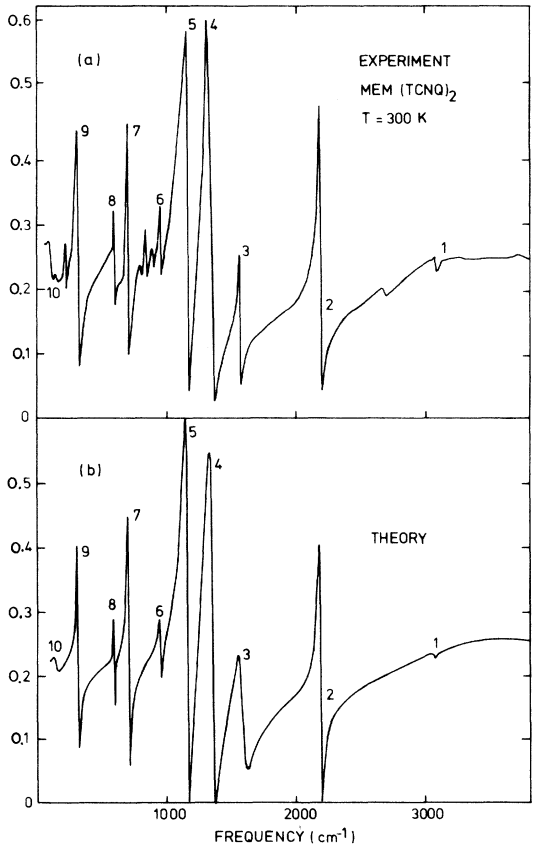


FIG. 5. Optical reflectance $R_{\parallel}$ as measured (upper curve) and calculated on the basic of the microscopic theory of Sec. II (lower curve).

TABLE I. $a_g$ vibrational modes of TCNQ ($cm^{-1}$).

| Mode | Isolated molecule [a] $(TCNQ)^0$ | Isolated molecule [a] $(TCNQ)^-$ | K–TCNQ [b] | MEM $(TCNQ)_2$ |
|---|---|---|---|---|
| 1 | 3048 | | | 3070 |
| 2 | 2229 | 2206 | 2225 | 2210 |
| 3 | 1602 | 1615 | 1632 | 1630 |
| 4 | 1454 | 1391 | 1395 | 1395 |
| 5 | 1207 | 1196 | 1206 | 1180 |
| 6 | 948 | 978 | 848 | 958 |
| 7 | 711 | 725 | 723 | 718 |
| 8 | 602 | 613 | | 597 |
| 9 | 334 | 337 | 333 | 324 |
| 10 | 144 | 148 | | 150 |

[a] After Girlando and Pecile, Ref. 16.
[b] After Rice, Lipari, and Strässler, Ref. 8.

culated reflectance is in remarkable agreement with the measured reflectance, as shown in Fig. 5.

The optimum values found for the parameters $\omega_{CT}$, $t^2/\omega_{CT}$ and $\gamma_e$ are $\omega_{CT} = 3250$ $cm^{-1}$ (0.4 eV), $t^2/\omega_{CT} = 768$ $cm^{-1}$, and $\gamma_e = 2000$ $cm^{-1}$ (0.25 eV). The $\pi$-MO hopping integral is thus found to be $t = 1580$ $cm^{-1}$ (0.195 eV). Also, since $\omega_{CT} = 2(t^2 + \Delta^2)^{1/2}$, we find the value of the total gap $\Delta = \Delta_c + \Delta_v^0$ to be $\Delta = 380$ $cm^{-1}$ (0.05 eV). According to Eq. (2.18), $\Delta_c$ may be found from $\Delta$ provided $E_p$ is known. We shall see that the experimental value we find for $E_p$ is $E_p = 688$ $cm^{-1}$ (0.085 eV). With this value for $E_p$, Eq. (2.18) yields $\Delta_c = 220$ $cm^{-1}$ (0.03 eV). The distortion gap $\Delta_v^0 = \Delta - \Delta_c$ is thus $\Delta_v^0 = 160$ $cm^{-1}$ (0.02 eV).

The values found for $\{\omega_\alpha\}$ and $\{\lambda_\alpha\}$ are listed in Tables I and II, respectively. In Table I the found set of values $\{\omega_\alpha\}$ are compared with those known for the isolated neutral[16] and singly charged[16] TCNQ molecule and those obtained[8] for the TCNQ anion in the dimerized simple salt K-TCNQ. The values of the EMV coupling constants $\{g_\alpha\}$ may be derived from the relation

$$\lambda_\alpha = \chi(0) g_\alpha^2/\omega_\alpha = 8(t^2 g_\alpha^2/\omega_{CT}^3 \omega_\alpha), \qquad (4.1)$$

where the second equality in (4.1) follows from Eq. (2.25). The resulting values for $g_\alpha$ are exhibited in Table III in which, for comparison are included the theoretical values of $g_\alpha$ calculated by Lipari *et al.*[9] Also included are experimental values of $g_\alpha$ previously obtained from optical-reflectance studies of[17] TEA$(TCNQ)_2$ and[8] K-TCNQ. From Tables I and III, the magnitude of $E_p = \sum_\alpha g_\alpha^2/\omega_\alpha$ for MEM$(TCNQ)_2$ is derived to be $E_p = 688$ $cm^{-1}$ (0.085 eV).

TABLE II. Dimensionless EMV coupling constants $\lambda_\alpha$.

| $\omega_\alpha$ ($cm^{-1}$) | $\lambda_\alpha$ | $\omega_\alpha$ ($cm^{-1}$) | $\lambda_\alpha$ |
|---|---|---|---|
| 3070 | $3.8 \times 10^{-4}$ | 958 | 0.004 |
| 2210 | 0.032 | 718 | 0.029 |
| 1630 | 0.104 | 597 | $2.5 \times 10^{-3}$ |
| 1395 | 0.104 | 324 | 0.058 |
| 1180 | 0.044 | 150 | 0.022 |

Table III shows that the values $\{g_\alpha\}$ deduced from the present measurements compare favorably with the theoretical calculations of Lipari *et al.*[9] Only for the two modes 8 and 6 do considerable differences arise. The small coupling constant $g_{10}$ associated with the higher-frequency CH stretch mode is reported here for the first time and its value $g_{10} = 44$ $cm^{-1}$ we consider to be in excellent accord with the theoretical estimate $g_{10} = 31$ $cm^{-1}$ of Lipari *et al.* The present reported values of $g_\alpha$ also agree generally well with those previously deduced for[17] TEA$(TCNQ)_2$ and[8] K-TCNQ. The differences probably reflect the differences in the quality of the respective experimental data and hence the data's susceptibility to theoretical analysis. The charge oscillation driven by the CH stretch mode, the dimensionless coupling constant associated with which is only of the order of $10^{-4}$, was neither observed in TEA$(TCNQ)_2$ nor K-TCNQ.

We note that several minor absorption features appear in the experimental spectrum which cannot be accounted for in terms of the expected dimer spectrum. In Fig. 4 these are labeled A through F. We believe the features C, E, and F arise from the IR active out-of-plane TCNQ modes ($b_{3u}$) which are known[16] to occur at the frequencies 859, 220, and 103 $cm^{-1}$, respectively. At this time we cannot offer an explanation of the three remaining features A, B, and D. [The feature A, in the region of 2700 $cm^{-1}$, is also observed[18] for TEA$(TCNQ)_2$, suggesting that it is associated with

TABLE III. Electron-molecular-vibration coupling constants $g_\alpha$ ($cm^{-1}$).

| Mode | Calculated[a] | K-TCNQ[b] | TEA(TCNQ)$_2$[c] | MEM(TCNQ)$_2$ |
|---|---|---|---|---|
| 1 | 31 | | | 44 |
| 2 | 423 | 589 | 339 | 350 |
| 3 | 1057 | 670 | 524 | 540 |
| 4 | 392 | 573 | 419 | 500 |
| 5 | 229 | 331 | 323 | 300 |
| 6 | 237 | 339 | 194 | 85 |
| 7 | 263 | 169 | 177 | 190 |
| 8 | 18 | | 105 | 50 |
| 9 | 194 | 177 | 234 | 180 |
| 10 | 78 | | 153 | 75 |

[a]After Lipari, Duke, Bozio, Girlando, and Pecile, Ref. 9.
[b]After Rice, Lipari, and Strässler, Ref. 8.
[c]After Rice, Pietronero, and Brüesch, Ref. 17.

the TCNQ stacks rather than the cations.]

If the values deduced above for $\Delta$ and $t$ are substituted into Eqs. (2.14) and (2.15) the ground-state wave function (2.12) of the distorted dimer is found to be

$$|E_-\rangle = 0.62\,|\phi_1\rangle + 0.79\,|\phi_2\rangle\,. \tag{4.2}$$

Consequently, the mean charge residing on the monomer 1 is $q_1 = 0.38e$, while that residing on the monomer 2 is $q_2 = 0.62e$. A rudimentary independent estimate of $q_1$ and $q_2$ may be obtained from the known dependence on charge $q$ of the length $l$ of the bridging carbon double bond (C) of the TCNQ molecule [Fig. 6(a)]. The lengths of the C bond reported in Refs. 19–21 for the respective charge occupations of 0, 0.5, and 1.0 provides the plot $q$ vs $l$ drawn in Fig. 6(b). From the x-ray structure studies of MEM(TCNQ)$_2$, Bosch and van Bodegom[2] have determined $l = 1.386$ Å for monomer 1 and $l = 1.399$ for monomer 2. With these values of $l$, Fig. 6(b) yields the estimates

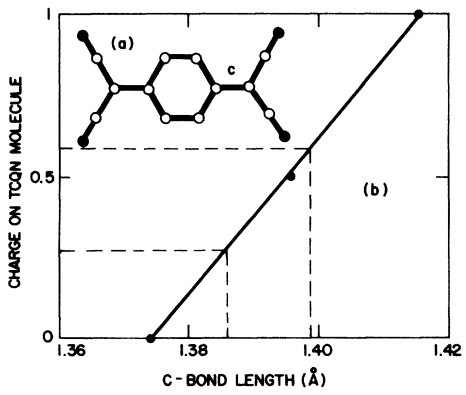


FIG. 6. Charge on TCNQ molecule as a function of the C-bond length (see text).

$q_1 = 0.26$ and $q_2 = 0.59$. The agreement with (4.2) is very reasonable in view of the obvious limitation inherent in the use of Fig. 6(b). For a more extensive discussion of the relation between the TCNQ internal bond lengths and the charge occupation we refer the reader to the paper by Flandrois and Chasseau.[22]

## V. CONCLUSIONS

This paper has investigated the nature of the unpaired electron states in the dimerized phase of the complex TCNQ salt MEM(TCNQ)$_2$. On the basis of polarized-optical-reflectance measurements and a theoretical analysis two basic conclusions have been arrived at. Firstly, each unpaired electron is localized on a dimeric TCNQ unit and occupies the two-site molecular orbital characteristic of the dimeric unit. The hopping integral $t$ specifying the intradimer interaction of the two underlying monomer $\pi$ MO's is experimentally found to be $t = 0.2$ eV. Secondly, the two-site molecular orbital involves molecular distortion which, interestingly, is driven by an initial (steric) site inequivalence of the individual TCNQ monomers. The energy of the bonding two-site MO relative to the energy of the noninteracting monomer $\pi$-Mo energy is

$$E_- = -(E_p/2) - [t^2 + (\Delta_c + \Delta_v^0)^2]^{1/2}\,,$$

where $E_p$ denotes the conventionally defined small-polaron binding energy, $\Delta_c$ the initial nonequivalence of the monomer site energies, and $\Delta_v^0$ the additional site nonequivalence due to molecular distortion. Experimentally, it is found that $E_p = 0.085$ eV, $\Delta_c = 0.027$, and $\Delta_v^0 = 0.02$ eV.

The localization of the unpaired electrons to the dimeric units is undoubtedly a consequence of the Coulomb repulsion between the unpaired electrons.

The latter suppresses the tendency to delocalization favored by the weak but finite interdimer interaction of the monomer $\pi$ MO's. We note that the Gröningen workers[3] have been able to explain the observed paramagnetism of MEM(TCNQ)$_2$ on the basis of the assumption that the dimerized TCNQ stack is equivalent to a half-filled Hubbard linear chain in which the atomic site is a TCNQ *dimer* and for which the on-site Coulomb repulsion $U'$ greatly exceeds the intersite hopping integral $t'$. Such a model may be expected also to account for the observed dc transport properties.[23] The verification of the dimeric localization of the unpaired electrons in MEM(TCNQ)$_2$ established in this paper provides a firm basis for the use of the latter model for this complex TCNQ salt. We note that the model dictates the existence of quite different energy gaps for the excitations responsible for electrical conduction, spin paramagnetism, and optical absorption. The gap for electrical conduction is essentially $U'$, namely, the energy required to thermally promote a doubly occupied and unoccupied dimer pair. For spin paramagnetism, the gap results from the weak interdimer antiferromagnetic exchange energy $4t'^2/U'$. The optical absorption gap, however, is the energy of the *intra*dimer charge-transfer excitation $\Omega_{CT}$.

## ACKNOWLEDGMENTS

It is a pleasure to acknowledge helpful discussions with D. B. Tanner, C. B. Duke, and J. S. Miller. Special thanks go to G. A. Sawatzky, B. Van Bodegom and A. Verwey who provided the beautiful single crystals used in this work and were responsible for stimulating our interest in MEM(TCNQ)$_2$. We thank Dr. R. W. Berg and Chemistry Department A, Technical University of Denmark, for the loan of the FS720 spectrometer. One of us (C.S.J.) acknowledges support from the Danish Natural Science Research Council. One of us (M.J.R.) was a guest of Nordita.

---

*Permanent address.

[1]P. I. Kuindersma, G. A. Sawatzky, and J. Kommandeur, J. Phys. C 8, 3005, 3016 (1975).

[2]A. Bosch and B. Van Bodegom, Acta Crystallogr. Sect. B 33, 3013 (1977).

[3]G. A. Sawatzky, S. Huizinga, and J. Kommandeur, in *Quasi-One-Dimensional Conductors II*, edited by S. Barisic *et al.* (Springer Verlag, Berlin, 1979), p. 34.

[4]S. Huizinga, J. Kommandeur, G. A. Sawatzky, K. Kopinga, and W. J. M. de Jonge, Ref. 3, p. 45.

[5]For a review, see I. F. Schegolov, Phys. Status Solidi A 12, 9 (1972).

[6]See, e.g., A. J. Berlinsky, J. F. Carolan, and L. Weiler, Solid State Commun. 15, 795 (1974).

[7]M. J. Rice, Solid State Commun. 31, 93 (1979).

[8]M. J. Rice, N. O. Lipari, and S. Strässler, Phys. Rev. Lett. 39, 1359 (1977).

[9]N. O. Lipari, C. B. Duke, R. Bozio, A. Girlando, and C. Pecile, Chem. Phys. Lett. 44, 236 (1976). See also M. J. Rice, N. O. Lipari, and C. B. Duke, Solid State Commun. 17, 1089 (1975).

[10]It could be viewed as a molecular Peierls distortion [cf. M. J. Rice, Phys. Rev. Lett. 37, 36 (1976)].

[11]For a discussion of electron-molecular-vibration coupling in TCNQ, see N. O. Lipari, M. J. Rice, C. B. Duke, R. Bozio, A. Girlando, and C. Pecile, Int. J. Quantum Chem: Quantum Chemistry Symposium 11, 583 (1977); M. J. Rice and N. O. Lipari, Phys. Rev. Lett. 38, 437 (1977); C. B. Duke, Ann. N. Y. Acad. Sci. 313, 166 (1978).

[12]Here, electronic energies are measured relative to the constant $E_0 - \frac{1}{2}E_p$.

[13]D. B. Tanner, C. S. Jacobsen, A. A. Bright, and A. J. Heeger, Phys. Rev. B 16, 3283 (1977).

[14]Y. Iida, Bull. Chem. Soc. Jpn. 42, 71 (1969); 42, 637 (1969).

[15]G. A. Sawatzky (private communication).

[16]A. Girlando and C. Pecile, Spectrochim. Acta A29, 1859 (1973).

[17]M. J. Rice, L. Pietronero, and P. Brüesch, Solid State Commun. 21, 757 (1977).

[18]A. Brau, P. Brüesch, J. P. Farges, W. Hinz, and D. Kuse, Phys. Status Solidi B 62, 615 (1974).

[19]R. E. Long, R. A. Sparks, and K. N. Trueblood, Acta Crystallogr. 18, 932 (1965).

[20]G. L. Ashwell, S. C. Wallwork, S. R. Baker, and P. I. Berthier, Acta Crystallogr. Sec. B 31, 1175 (1975).

[21]M. G. Kaplunov, Fiz. Tverd. Tela (Leningrad) 20, 1529 (1978) [Sov. Phys.–Solid State 20, 881 (1978)].

[22]S. Flandrois and D. Chasseau, Acta Crystallogr. Sec. B 33, 2744 (1977).

[23]E. M. Conwell, A. J. Epstein, and M. J. Rice, in *Quasi-One-Dimensional Conductors I*, edited by S. Barisic *et al.* (Springer Verlag, Berlin 1979), p. 204.